Tellus (1999), 51B, 194–209
Printed in UK – all rights reserved

TELLUS
ISSN 0280–6495

Model simulations of anthropogenic-CO_2 transport to an Arctic monitoring station during winter

By MAGNUZ ENGARDT[1]* and KIM HOLMÉN, *Department of Meteorology, Stockholm University, S-106 91 Stockholm, Sweden*

(Manuscript received 18 November 1997; in final form 22 September 1998)

ABSTRACT

We describe, and use, a limited area, 3-dimensional transport model. The model domain is located over the Arctic, but includes the majority of the anthropogenic CO_2 emissions in western and eastern Europe, which together make up about 1/3 of the global CO_2 emissions. The model is run for several winter periods, using anthropogenic CO_2 emissions only, and the results are compared with independent CO_2 measurements taken at a monitoring station on Spitsbergen in the high Arctic. We show that the initial concentrations and boundary values of the domain are not crucial for the results, and conclude that most of the measured variability above the winter baseline in CO_2 at the Arctic monitoring station emanates from recent CO_2 sources within the model domain. From the observed small spatial variability in the monthly mean atmospheric CO_2 mixing ratio in the north Atlantic region, we assume that there is only little net exchange between the atmosphere and ocean during the studied periods. Based on the co-variation between CO_2 and particulate mass, we hypothesise that most of the measured CO_2 variability is due to anthropogenic fossil fuel emissions, although we can not rule out a biogenic CO_2 component. Using the transport model, we compare different estimates of fossil-fuel consumption in the mid-latitudes. We find that the industrial centres and the surrounding gas-fields in the lower-Ob region (60°–72°N, 65°–80°E) occasionally have a much larger impact on the CO_2 measurements at Spitsbergen than follows from a recent CO_2 emission inventory. This implies that there may be an overlooked CO_2 source in this region, possibly flaring of gas.

1. Introduction

Carbon dioxide (CO_2) is injected to the atmosphere from several different sources, both natural and anthropogenic. Although the natural CO_2 fluxes are greater than the anthropogenic by more than an order of magnitude, atmospheric CO_2 is increasing due to human activities, raising concern about possible future climate change. Apart from the atmospheric burden of CO_2, the burning of fossil fuel has traditionally been recognised as the least uncertain of all terms in the atmospheric carbon budget. However, there are still uncertainties, both regarding its magnitude, and its spatial distribution. In this study, we describe a situation where anthropogenic CO_2 emissions are comparable, or larger, than the natural CO_2 fluxes. By identifying such periods we may quantify the actual CO_2 emissions and thus indicate errors in current estimates of anthropogenic CO_2 emissions.

In winter and early spring the Arctic troposphere is episodically intruded by tongues of anthropogenic pollution from the mid-latitudes, so called "Arctic haze". The homogenous surface conditions and the great atmospheric stability cause these tongues to be confined to well defined layers, which, when reaching a monitoring station,

[1] Corresponding author.
* Current affiliation: Swedish Meteorological and Hydrological Institute, S-601 76 Norrköping, Sweden. E-mail: magnuz.engardt@smhi.se.

are recorded as periods with enhanced concentrations of several anthropogenic trace species. The episodes, lasting from a few hours to a few days, generally have distinct start and stop times and feature elevated concentrations of both aerosol particles, and long-lived gases such as carbon dioxide (CO_2) and methane (CH_4) (Hansen et al., 1989; Worthy et al., 1994). From geographical and circulation considerations it is obvious that the anthropogenic emissions in Eurasia in general, and in northern Siberia in particular, must have the largest impact on the pristine Arctic atmosphere (Barrie, 1986).

In this study, we use a 3-dimensional atmospheric transport model to simulate the advection of anthropogenic CO_2 into and out of the Arctic during selected winter periods. The transport model is driven by archived observed meteorology, with spatial and temporal resolution fine enough to resolve synoptic events at a monitoring station. We chose to investigate a few periods that were identified as typical examples of episodic CO_2 pollution at a monitoring station on Spitsbergen, in the Norwegian high Arctic.

In Section 2, we briefly describe the monitoring station on Spitsbergen and the CO_2 measurements performed there. Section 3 provides a short description of the transport model. In Section 4, we compare measured and modelled CO_2 mixing ratios at the Spitsbergen monitoring station and argue that most of the day-to-day variability in CO_2 is due to relatively recent anthropogenic emissions. We show that it is possible to neglect the CO_2-fluxes through the model boundaries during winter, and that the initial conditions are of minor importance after 10–20 days of integration. Because the influence of natural CO_2-fluxes seem to be outweighed by anthropogenic emissions during winter, we use the tongues of Arctic haze as probes for anthropogenic CO_2 emissions. In Section 5, we use 2 different CO_2 emission estimates and compare their respective influence on the air at Spitsbergen. Section 6 concludes the paper with a summary of the results.

2. Atmospheric CO_2 data from the Norwegian high Arctic

Continuous CO_2 measurements, utilising non-dispersive infra-red technique with a UNOR 4N instrument (H. Maihak AG, Hamburg), have been ongoing near Ny-Ålesund, Spitsbergen, since 1988, and on Zeppelinfjellet since 1990 (Holmén et al., 1995; Engardt et al., 1996). The Zeppelinfjellet station, part of the "Ny-Ålesund International Arctic Research and Monitoring Facility", is an excellent location for measuring background CO_2. The monitoring station is placed on a barren mountain ridge (ca. 475 m above m.s.l.), a few km south of the village of Ny-Ålesund. The station is only accessible for authorised scientists and technicians through an electrically powered cable car starting from the base of the mountain. Ny-Ålesund (<50 inhabitants in winter) is situated in the valley of Kongsfjorden on north-western Spitsbergen at 79°N, 12°E. Apart from the 3–4 Norwegian and Russian settlements (about 1000 inhabitants each) $\sim$100 km further south, the nearest human activities are located at least 1000 km to the south. Most parts of Spitsbergen are covered by glaciers and the sparse vegetation that grows in the fjord valleys during summer probably has a negligible effect on the current CO_2 measurements. We consider all hours and all wind-directions representative for background conditions. The CO_2 mixing ratios discussed in this work are reported in the WMO X85 mole fraction scale.

Weekly samples, analysed for CO_2 at NOAA/CMDL in Boulder, Colorado, have been collected at the Zeppelinfjellet site since February 1994 (NOAA/CMDL, 1996) and at a nearby sea-level site by the National Institute of Polar Research (NIPR) since 1991 (Yamanouchi et al., 1996). Comparisons between our continuous data and the NOAA/CMDL weekly data show correspondence, within $\pm$0.3 ppmv (Holmén et al., 1995).

3. Transport model description

3.1. Basic structure

MATCH (Multiple-scale Atmospheric Transport and CHemistry modelling system) is an "off-line", 3-dimensional, Eulerian transport model, developed at the Swedish Meteorological and Hydrological Institute (SMHI). The model has been thoroughly described in Robertson et al. (1998), where a number of test-simulations also demonstrate its general performance. A summary

of the current model set-up will be given in the following.

The resolution in MATCH is determined by the input meteorological data. In this study, the model is driven by the initialised analysis of the European Centre for Medium Range Weather Forecast (ECMWF), available every 6 h. The data are first spatially interpolated onto the rotated latitude/longitude grid that defines the model domain (cf. Fig. 1 or Fig. 3), and next linearly interpolated in time to 1 h resolution. The rotation of the grid proceeds through moving the "poles" of the global grid such that the "Equator" of the rotated latitude/longitude grid lies in the middle of the chosen domain. This results in a nearly uniform grid, without a singularity at the real North Pole. The horizontal resolution in this study is $1^\circ \times 1^\circ$ (i.e., ca. 110 km × 110 km), and the advection time-step 5 min. The domain covers 77×68 grid cells in the horizontal while the vertical structure is identical to the original data, except at the top boundary, which we set to 10 hPa. The ECMWF-data is calculated in the spectral domain with a T213 truncation, and 31 unequally distributed layers in the vertical (cf. Fig. 6). The vertical dimension is η-coordinates, from which the pressure, p_k, at each model interface is obtained through

$$\eta_k = \frac{p_k}{p_s}, \tag{1a}$$

$$p_k = \alpha_k + \beta_k p_s, \tag{1b}$$

α_k and β_k are constants and p_s is the surface pressure in Pa. Index k refers to one of the $(n\text{lev} + 1)$ layer interfaces, where $n$lev is the number of model layers.

Vertical winds are calculated in MATCH, after an adjustment of the horizontal wind, by integrating the continuity equation for air, from the surface ($\eta = \eta_1 = 1$) to the top of the model domain ($\eta = \eta_{32} = 1000/p_s$), with the boundary condition $\partial\eta_k/\partial t = 0$ at η_1 and at η_{32}. The adjustment is necessary in order to balance the wind field after the spatial and temporal interpolation of the original data. The adjustment proceeds through an iterative correction (equally in all model layers) of the magnitude of the horizontal wind until the surface pressure tendency calculated from the column divergence over each grid cell equals the tendency of surface pressure achieved from a linear interpolation of the surface pressure (for details, see Heimann and Keeling, 1989).

3.2. Advection

In MATCH, the continuity equation for the mixing ratio of the advected species (μ) is solved in an Eulerian frame-work:

$$\frac{\partial \mu}{\partial t} = -\nabla \cdot (\mu v) + Q - S, \tag{2}$$

where v is the 3-dimensional wind-vector (u, v, w). Q is the source and S the sink for the species. The emissions can be discharged in any model layer and represent an instantaneous increase of the mixing ratio in a grid cell just prior to the advection is calculated.

The horizontal advection is calculated directly from the input meteorological data while the vertical advection is split into a mean- and a turbulent term:

$$\nabla \cdot (\mu v) = \nabla_H \cdot (\overline{\mu v_H}) + \frac{\partial(\overline{\mu w})}{\partial z} + \frac{\partial(\overline{\mu' w'})}{\partial z}. \tag{3}$$

Lines above factors denote temporal grid cell averages and primes denote deviations from the mean values. ∇_H is the horizontal gradient operator $(\partial/\partial x, \partial/\partial y, 0)$ and v_H is the horizontal wind-vector $(u, v, 0)$. Combining (2) and (3) yields the continuity equation for CO_2 in flux form:

$$\frac{\partial \mu}{\partial t} = -\left(\frac{\partial \overline{F_x}}{\partial x} + \frac{\partial \overline{F_y}}{\partial y} + \frac{\partial \overline{F_z}}{\partial z} + \frac{\partial(\overline{\mu' w'})}{\partial z}\right) + Q - S. \tag{4}$$

where $\overline{F_i}$ represent the net kinematic flux of CO_2 across the cell boundaries with the mean wind in the i-direction (x, y, or z). The flux is calculated by fitting a polynomial, P_i, to the one-dimensional distribution of μ around each grid cell and then advect P_i with the wind at the grid cell boundaries (Tremback et al., 1987). For the horizontal advection a fourth order polynomial is used to describe the distribution of CO_2; for the vertical advection we use a second order polynomial. The complete, 3-dimensional, advection with the mean wind proceeds by first calculating the three advection terms (using the same, non-updated CO_2 field), before updating the mixing ratios in each grid cell. The scheme is similar to what Bott (1989a,b) proposed for one-dimensional advection, using time-splitting for multi-dimensional advection.

3.3. Boundary layer parameterisations

Diurnal and spatial variations of the turbulent flux in the planetary boundary layer are parameterised as a function of a vertical exchange coefficient K_Z, and from the local vertical gradient of μ:

$$\overline{\mu' w'} = -K_Z \frac{\partial \mu}{\partial z}. \quad (5)$$

The exchange coefficient is dependent on the bulk properties of the planetary boundary layer (Holtslag et al., 1990):

$$K_Z = k w_i z \left(1 - \frac{z}{z_{\mathrm{PBL}}}\right)^2; \quad (6)$$

k is the Von Karman constant, w_t a characteristic turbulent velocity scale; z is the height above the surface and z_{PBL} is the diagnosed height of the planetary boundary layer. z_{PBL} is a function of the temperature- and wind-gradients close to the ground, and also dependent on cloud cover, surface type and roughness. For the convective boundary layer, we use a formulation for z_{PBL} based on a bulk Richardson number as proposed by Holtslag et al. (1995). For neutral and stable conditions we follow Zilitinkevich and Mironov (1996) (their eq. (30)).

The boundary layer height and the profile of the vertical exchange coefficient over each grid cell, determine the effectiveness of the near surface mixing. The current version of MATCH has no sub-grid vertical diffusion outside the planetary boundary layer, nor an inclusion of parameterised convective transport in clouds. Studies with passive tracers (Robertson et al., 1998) have shown realistic simulations of radon-222 in the lower troposphere. Lack of data, have, so far, hampered us from judging the performance of the model in the middle and upper troposphere.

4. Experimental set-up and sensitivity tests

4.1. Source function

The primary CO_2 emission inventory is described in Andres et al. (1996) (henceforth A96), and consists of a global $1^\circ \times 1^\circ$ map of anthropogenic CO_2 emissions, valid for the year 1990. A96 calculate national fossil fuel CO_2 emissions using relevant emission factors together with energy statistics from the United Nations and cement production data from US Bureau of Mines. A96 spread the emissions within each country based on population densities. The global total of 5.812 Pg C year^{-1} ($=5.8 \times 10^{15}$ g carbon per year) in the A96 inventory is lower than the Marland et al. (1994) estimate of 6.098 Pg C for 1990 due to the deliberate omission of bunker-fuel consumption and production of non-fuel products. It is also likely that the anthropogenic CO_2 emissions are larger during winter compared to summer (Rotty, 1987; Levin et al., 1995). However, while the anthropogenic CO_2 emissions from western Europe have been approximately steady since the late 1970s, the emissions from Russia and Eastern Europe have probably decreased significantly since the late 1980s (Marland et al. 1994). Due to large uncertainties in these numbers, we keep the emissions constant at their 1990 values. Fig. 1 shows the magnitude, and spatial distribution, of the CO_2 emissions in the model domain. CO_2 is emitted into the lowest model layer without diurnal or seasonal cycle, and the total emissions within the model domain are 1.9 Pg C year^{-1}. We have also performed sensitivity tests where we released all emissions in layer 2 (50–200 m). Although this must be regarded as an upper limit of where the emissions are actually released, the resulting CO_2 mixing ratios in most of the model domain were only marginally different. In the following simulations, we neglect all sources for CO_2 except the anthropogenic emissions. We also neglect any sinks for atmospheric CO_2 that may occur in the domain during the studied period. Below we will show that the assumptions regarding Arctic sources and sinks of CO_2 during winter are acceptable.

4.2. Initial and boundary conditions

To investigate the significance of the initial and boundary conditions, we performed a number of tests where we initialised the model with different conditions. In the following, we describe some of these tests and discuss the results in light of the resulting time-series at the Zeppelinfjellet location.

Fig. 2b shows CO_2 mixing ratios at Zeppelinfjellet in January and February 1993. The measurements reveal typical winter conditions with episodes of elevated CO_2 roughly once every week. The start- and stop-times of these events

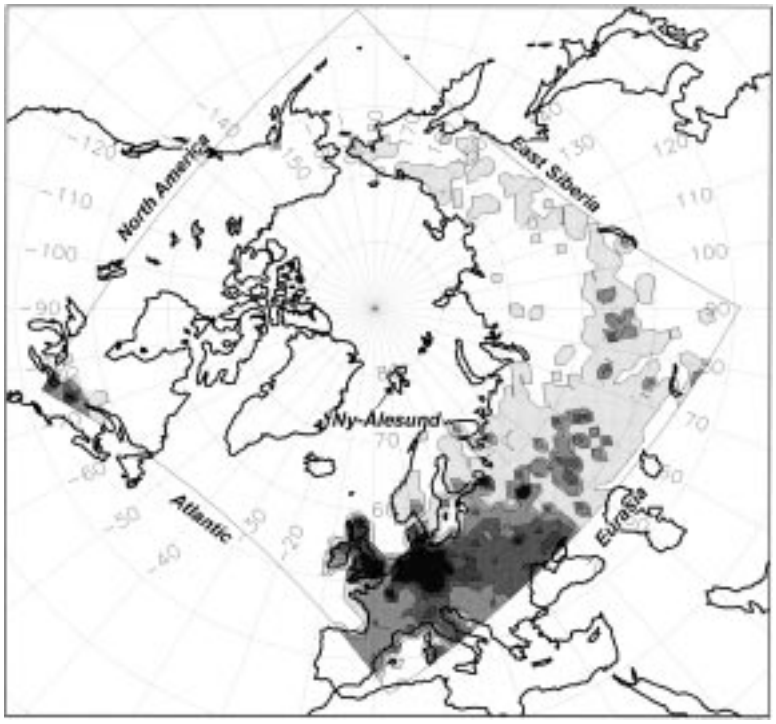

Fig. 1. CO_2 emissions from Andreas et al. (1996) mapped to the MATCH domain. Different grey shadings indicate the intensity of the emissions. Isolines at 0.01, 0.15, 0.25, 0.5, 1.0, and 1.5 g C m^2 day^{-1}. The lateral boundaries discussed in Subsection 4.2, as well as Ny-Ålesund's location on the west coast of Spitsbergen are also indicated on the map.

are well defined and the magnitude of the CO_2 excursions is several ppmv.

The solid line in Fig. 2a is the result from the "standard run" with zero CO_2 in the domain at start and no influx through the boundaries. The dotted line is the result from an experiment where we used the final CO_2-field from the standard run (i.e., after 50 days of integration), as initial- and boundary condition, in all 31 model layers. The dash-dotted line shows the result from a hypothetical scenario where we assigned all continental grid cells, from the surface to the top of the domain, 10 ppmv, while oceanic cells had 0 ppmv at start. The dashed line, finally, depicts the results when we initialised the model with monthly mean mixing ratios from a course-grid global CO_2 model (M. Heimann, personal communications*),* and where we updated the boundaries every 1 h with interpolated monthly data from the global model. Influx of CO_2 through the boundaries occurred in the three latter experiments and was dependent on the CO_2 mixing ratio at the boundaries (Robertson et al., 1998). All four model simulations used the A96 source function described in Subsection 4.1. Although the initial conditions and boundary values vary considerably, the resulting time-series at Zeppelinfjellet in February 1993 appear mainly as parallel shifted. This implies that the background mixing ratio is determined by the amount of CO_2 on the model-boundaries, while the synoptic variability (i.e., the "spikes") are generated by the sources within the model domain and must be of recent origin. This should also be expected from the measurements alone, since the well-defined start- and stop times of the spikes cannot be maintained if mixing has been given time to act.

The soundness of assigning homogenous initial conditions is also partially supported by the small temporal and spatial gradient of CO_2 actually recorded in the region during this period (NOAA/CMDL, 1995). Excluding the measure-

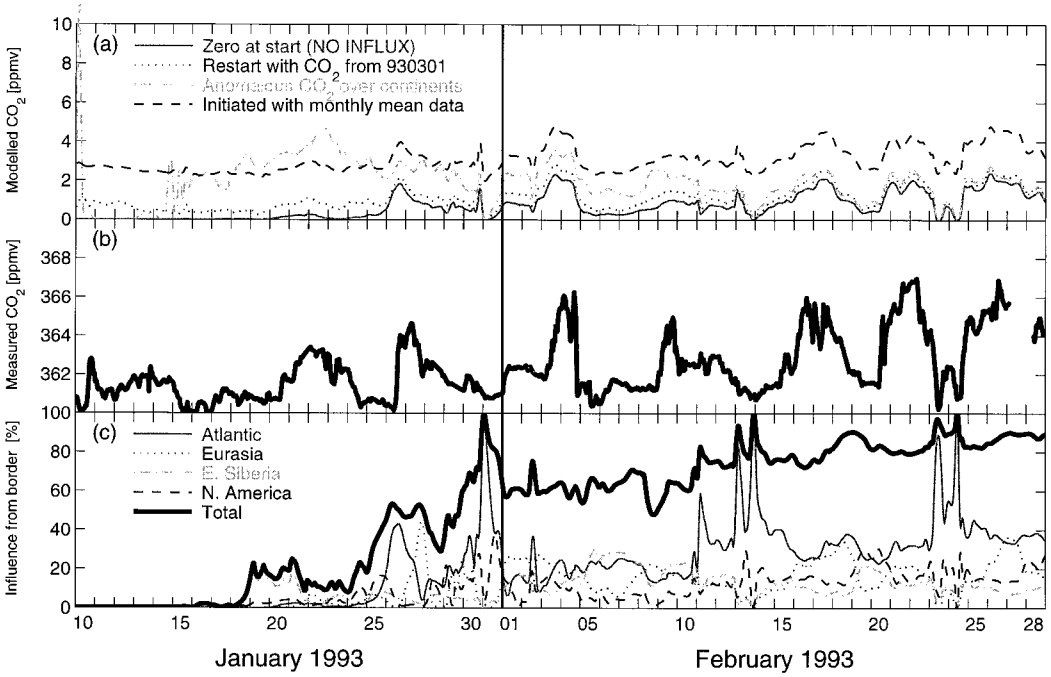

Fig. 2. Measured and modelled CO_2 at Zeppelinfjellet's location in January and February 1993. (a) Sensitivity test where the interior and the boundaries were assigned completely different conditions, and the A96 emissions (1.9 Pg C $year^{-1}$) were used. (b) Measured hourly median CO_2 for comparison. (c) Relative influence of each of the lateral boundaries at Zeppelinfjellet's location plus the total influence (thick solid lines) from all four boundaries.

ments performed in the Baltic, near the European CO_2 emissions, the remaining seven flask sampling stations in operation within the model domain had monthly mean mixing ratios of (minimum–maximum) 359.0–362.6 ppmv and 359.5–362.6 ppmv for January and February 1993, respectively.

To specifically investigate the importance of the model boundaries, we next performed simulations where each one of the four lateral boundaries was assigned μ_0 ppmv CO_2, from the surface to the top of the domain. The other boundaries and the interior of the model were initialised with 0 ppmv; no sources were present during these integrations. The signal in Fig. 2c is the combined effect of advection and mixing within the model domain, and represents the relative influence, at Zeppelinfjellet's location, of the respective boundary compared to the other three boundaries and the initial mixing ratios. As expected, the boundary located over the Atlantic (thin solid line in Fig. 2c) makes the greatest imprint on the air at Spitsbergen. The signal from the other three boundaries only rarely reach even a third of their initial values, reflecting the greater mixing following the longer transport times to Zeppelinfjellet. None of the measured spikes in CO_2 (cf. Fig 2b) occur in air that is markedly influenced by the boundary. Rather, when the signal from the Atlantic boundary penetrates undiluted all the way to Spitsbergen we always measure a minimum in the CO_2 mixing ratios at Zeppelinfjellet. The absolute values measured at Zeppelinfjellet during these minima (360–361 ppmv) are similar to what was recorded by NOAA/CMDL in the north Atlantic during this period (NOAA/CMDL, 1995), thus indicating only little net air-sea exchange of CO_2 in the region during this time. Finally, we note, that after 20 days of integration, typically about 60% of the signal modelled at Spitsbergen is due to "new" air coming from the model's boundaries. After 50 days, this number has increased to 90%.

Based on these results, we conclude that there is no stagnant Arctic air mass where anthropo-

genic pollutants are gradually accumulating throughout the winter. Rather, there seem to be a vigorous transport of air across the polar region, carrying polluted air into and out of the Arctic. The tongues of Arctic haze are swept into the region from the mid-latitudes by migrating cyclones on the Arctic-front. The age of the pollution in these tongues is, at least at Spitsbergen, typically no more than a week.

4.3. *Alternative source function*

Above we used a recent compilation of anthropogenic CO_2 emissions (i.e., A96). We showed that the resulting time-series at Zeppelinfjellet were not dependent on the initial conditions in the domain or on the boundary values of the model. Still the modelled anomalies at Spitsbergen were too small compared to the measurements (cf. solid lines in Fig. 2a and Fig. 2b). Several reasons can cause a too small anomaly. Both vertical and horizontal diffusion or a coarse resolution can give such effects. The shape of the protruding CO_2 tongues (not shown, but manifested in the rapid changes of modelled CO_2 at Zeppelinfjellet) is such that the horizontal effects are unlikely. Vertical effects will be discussed below.

Still another reason for the discrepancy between the measurements and the modelled time-series at Zeppelinfjellet can arise from errors in the emission field. Above, we used the reported A96 emissions valid for 1990 without correcting for seasonal or temporal trends. The winter-time emissions may be 10–30% larger than the fluxes derived from the annual mean emissions (Rotty, 1987; Levin et al., 1995). However, it is likely that the Russian and east European emissions have plunged 15–20%, between 1990 and 1993 while the west European emissions have decreased by 2–3% (Marland et al., 1998). Thus, while these numbers are highly uncertain, it appears that they, to a first approximation, offset each other.

To test an alternative emission field, we utilise a global distribution of anthropogenic sulphur (sulphur dioxide and sulphate; SO_x) emissions recently compiled by Benkovitz et al. (1996). Their data are a synthesis of a number of detailed regional estimates of sulphur emissions, which all explicitly consider point sources of SO_x before spreading the remaining emissions within each country. We believe that while it is possible to determine national CO_2 emissions from economical statistics with some confidence, it is not straightforward how to distribute them geographically. In central and northern Siberia, for instance, considerable industrial activities are located in certain, relatively sparsely populated, industrial centres. Although anthropogenic SO_x may be released to the atmosphere without accompanying CO_2 we believe that is important to take the "point-sources" in Siberia into consideration. The Benkovitz et al. SO_x-emissions will serve as a first approximation for the CO_2-emissions from these regions. In this study, we linearly scale the Benkovitz et al. $1^\circ \times 1^\circ$ map of SO_x emissions such that the CO_2 emissions within the MATCH domain are the same as in the A96 scenario, namely 1.9 Pg C year^{-1}.

Fig. 3 shows the alternative SO_x-derived emission estimate. In the SO_x-derived field there are several "point-sources" with large CO_2 emissions, east of 70°E. Compared to the A96 inventory the maximum emissions in central Europe are now shifted eastward, while the emissions in southwestern Europe are slightly smaller.

5. Results

In this section, we discuss the simulations during two different winter periods. The emphasis will be on the 1993 period, which was also used for the sensitivity tests above. We find that the two periods differ in terms of circulation patterns. During the first period the polluted air stemmed from Siberia while during most of the second it arrived from western Europe. However, in none of the cases did the simulations using the SO_x derived source function show worse resemblance with the measurements than those using the original A96 inventory.

5.1. *February 1993*

Fig. 4a shows CO_2 mixing ratio and the aerosol particle scattering coefficient σ_{sp}, at Zeppelinfjellet in February 1993. σ_{sp} is by definition high in Arctic haze and also proportional to particulate sulphate mass (Waggoner and Weiss, 1980; Barrie and Hoff, 1985). The high correlation between measured CO_2 and σ_{sp} is therefore by itself a strong argument for using the detailed (i.e., includ-

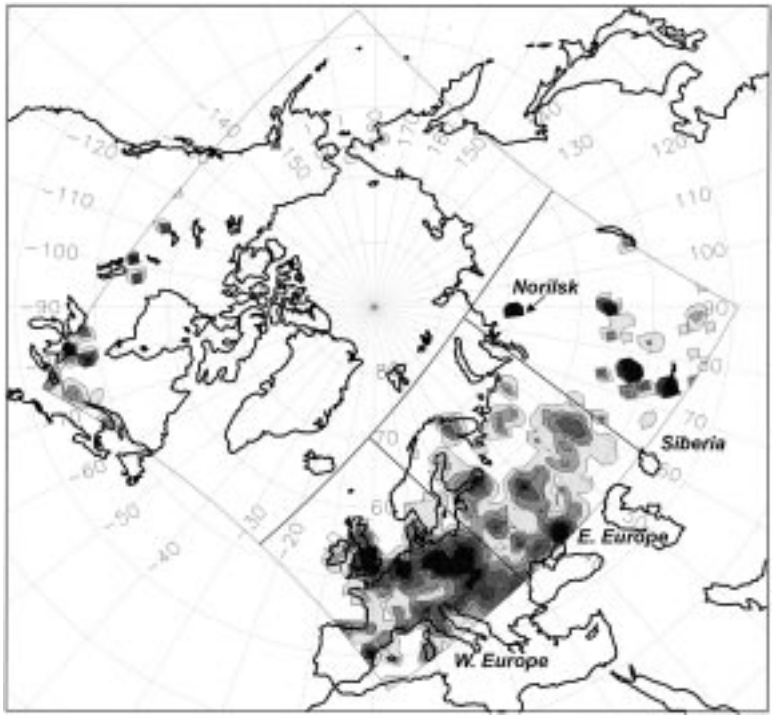

Fig. 3. Scaled SO_x emissions from Benkovitz et al. (1996) mapped to the MATCH domain. Different grey shadings indicate the intensity of the emissions. Isolines at 0.01, 0.15, 0.25, 0.5, 1.0, and 1.5 g C m^2 day^{-1}. Also indicated are the borders between the three Eurasian sub-regions (Western Europe, Eastern Europe, and Siberia) and Norilsk, which are discussed in the text.

ing point sources) SO_x source-inventory for distributing the CO_2 emissions, or any other Arctic haze precursor.

In Fig. 4b we compare the modelled results at the Zeppelinfjellet location when using the A96 inventory and the alternative, SO_x-derived source function. In this, and all following simulations, the CO_2 mixing ratios in the domain are set to zero at the beginning of the integrations and the lateral boundaries are treated such that the incoming air is always free of CO_2. The experiments thus simulate the changes in CO_2 brought about by the specified anthropogenic sources of CO_2 within the domain. In these simulations the model was run from 10 January through 28 February 1993, the results are plotted after 22 days of "harmonisation".

When using the emissions from A96 we previously noted that the timing of most of the positive excursions (the "spikes") was successfully simulated while the magnitude was often underestimated. If we instead use the distribution of the SO_x-emissions as a proxy for the location of the anthropogenic CO_2 sources, the magnitude of the modelled anomalies corresponds better with the measurements, see Fig. 4b. The detailed structure of the simulated time-series and the excellent correlation in timing between the measured and modelled anomalies lend credibility to the horizontal advection scheme in particular, but also to other features of the transport model, such as the near surface mixing and the specified source-function.

Although the simulated CO_2 anomalies at the end of February 1993 only attain half of the measured magnitude at these dates, the correspondence with the measurements is surprisingly good. Several of the point sources for SO_x emissions in Siberia emanate from metallurgic activities (Benkovitz et al., 1996) which should not be accompanied with high CO_2 emissions but will affect σ_{sp} strongly. We suspect that the correlation

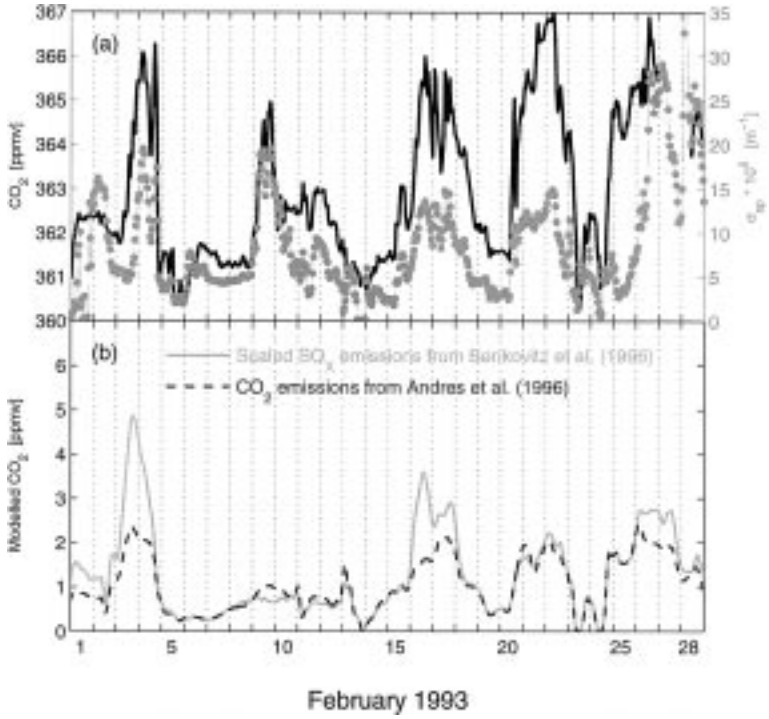

Fig. 4. CO_2 and σ_{sp} (the aerosol particle scattering coefficient at 550 nm) at Zeppelinfjellet in February 1993. (a) Measured hourly median CO_2 mixing ratio (solid line) and measured hourly median σ_{sp} (dotted line). (b) Modelled CO_2 mixing ratio after 22 days of "harmonisation". Solid line is the results when using the scaled SO_x-emissions from Benkovitz et al. (1996), dashed line is with CO_2-emissions from Andres et al. (1996). Total CO_2 emissions in model domains is 1.9 Pg C year^{-1} in both simulations.

between CO_2 and aerosol particle concentration is partly coincidental; there are often several, potentially important, activities going on in the same regions. We suggest that, flaring of gas is a significant but overlooked CO_2 source in the former Soviet Union (FSU). This hypothesis is also supported by the high correlation between combustion products such as CO_2 and aerosol-particles with CH_4 (Conway and Steele, 1989; Trivett et al., 1989) which probably have a large non-combustion source from leakage in connection to natural gas exploitation and transportation (Müller, 1992). Another possibility is that the air arriving at Spitsbergen also has taken up some respiratory CO_2 released from continental Eurasia. Zimov et al. (1996) recently showed that the CO_2 efflux from parts of Siberia can be substantial even during winter. In their study, the average wintertime CO_2 efflux was 89 g C m^{-2} year^{-1}. It is, however, not likely that their data are representative of a larger region since, at their plots, the tundra was not in balance with the atmosphere but acted as a net source for CO_2 with the magnitude 150–300 g C m^{-2} year^{-1}. Because all the CO_2 spikes in February 1993 were accompanied by high σ_{sp} we do not believe that biogenic CO_2 efflux in Eurasia was the main cause for the observed CO_2 anomalies.

The measured peak in CO_2, and σ_{sp}, on February 9–12 is not simulated with any of the emission estimates and we may speculate on its origin. The sensitivity tests presented in Fig. 2a indicate that it is not likely the manifestation of an "old CO_2 anomaly" floating around in the region. Furthermore, Fig 2c shows that during this episode the air is not coming directly from the borders of the domain, and it is therefore not likely that the spike originates from CO_2 sources in eastern Asia (i.e., China or Japan) or North America. Vertical mixing is also an unlikely can-

didate for the CO_2 anomaly, since CO_2 mixing ratios are generally decreasing with altitude over the northern hemisphere in winter (Bolin and Bischof, 1970). Local contamination, finally, can be excluded due to the small hourly variability (not shown) and the length of the episode. The most likely explanation is therefore an omitted source within the model domain. The sharpness of the spike is an indication of a relatively recent (i.e., Eurasian) source. Three-dimensional trajectories (McGrath, 1989), calculated 5 days backwards, suggest that the air at Zeppelinfjellet on 9 February, originates from Siberia, east of 120°E, a region where none of the utilised inventories suggest any significant CO_2 emissions. There is some gas and coal exploitation in the Vilyuysk-Yakutsk region (ca. 62°N, 130°E) in addition to the extensive gold and diamond prospecting there. We suggest that this area is the source for CO_2, and other anthropogenic pollutants at Zeppelinfjellet during this particular episode. Pacyna et al. (1985) mentioned Yakutsk as one of the emissions regions in the FSU which might affect the atmospheric concentration of trace species at Ny-Ålesund during March-April 1983, and our study gives an indication that this may be the case, also during other periods.

In order to investigate which geographical regions that have the greatest impact on the CO_2 measurements at Zeppelinfjellet in February 1993, we divided the SO_x-derived Eurasian emissions into three sub-regions (cf. Fig. 3), and performed experiments were we retained only the emissions in each one of these regions. As evident from Fig. 5b, the sources in Siberia have a very large impact on the measurements at Zeppelinfjellet, despite the fact that they only comprise $\sim$15% of the amount of CO_2 emitted in the MATCH domain.

The Siberian emissions may be even further split up to illustrate the importance of a small distinct region. Fig. 5c displays the result of a simulation where all sources but Norilsk (69°N, 88°E) were masked away. As can be seen, the emissions from Norilsk often make up half, or more, of the modelled signal during the pollution events at Zeppelinfjellet during this month. The ultra-high SO_x emissions from Norilsk mostly emanate from the roasting of copper and nickel ores and are not accomplished by high CO_2 emissions. However, in the adjacent lower-Ob region (60–72°N, 65–80°E), there are huge gasfields (A.G. Ryaboshapko, personal communications) and we suggest that this specific area may be one of the main sources for the haze layers measured throughout the Arctic in winter. The total CO_2 emissions from Norilsk deduced from the SO_x scaling, and supported by this study, is 0.1 Pg C year^{-1} or 8% or the FSU emissions for 1990.

Apart from an anomaly on 13 February, when a surge with moderately polluted air from western Europe affects Spitsbergen, the emissions from the different regions most often result in positive anomalies at Zeppelinfjellet on the same dates. This is intriguing and implies that the transport of anthropogenic pollutants into the Arctic, during this month, most often took the route from Europe through western Siberia, passing over the Gulf of Ob, before entering the Arctic basin. It is therefore a definite possibility that the different trace species that are enhanced during Arctic haze episodes, may have different source regions but are mixed en route to form the polluted tongues that eventually reach the Arctic as distinct haze layers (Khalil and Rasmussen, 1984). Also, any biogenic CO_2 from northern Siberia might arrive simultaneously, and indistinguishable, from the anthropogenic CO_2 in Arctic Haze.

5.2. *Vertical profiles*

In order to demonstrate the performance of MATCH in the vertical, we show in Fig. 6, calculated profiles of CO_2 mixing ratios over two Arctic monitoring stations. Over Zeppelinfjellet, the calculated maximum mixing ratios are virtually always confined to the lowest model layers, while over Alert in the Canadian Arctic, the tongues of anthropogenic pollution are most often located at a few km height, yielding smaller surface anomalies.

The simulated vertical profiles can be compared with the measurements performed in the Arctic troposphere during AGASP-II and AGASP-III (Conway and Steele, 1989; Conway et al., 1993). In the AGASP-data they found CO_2 increases of 1–4 ppmv in haze layers which were encountered up to ca. 5 km height. The sampling was specifically aimed at determining CO_2 and other gases in Arctic haze, but suffered from a relatively low vertical resolution. Other studies

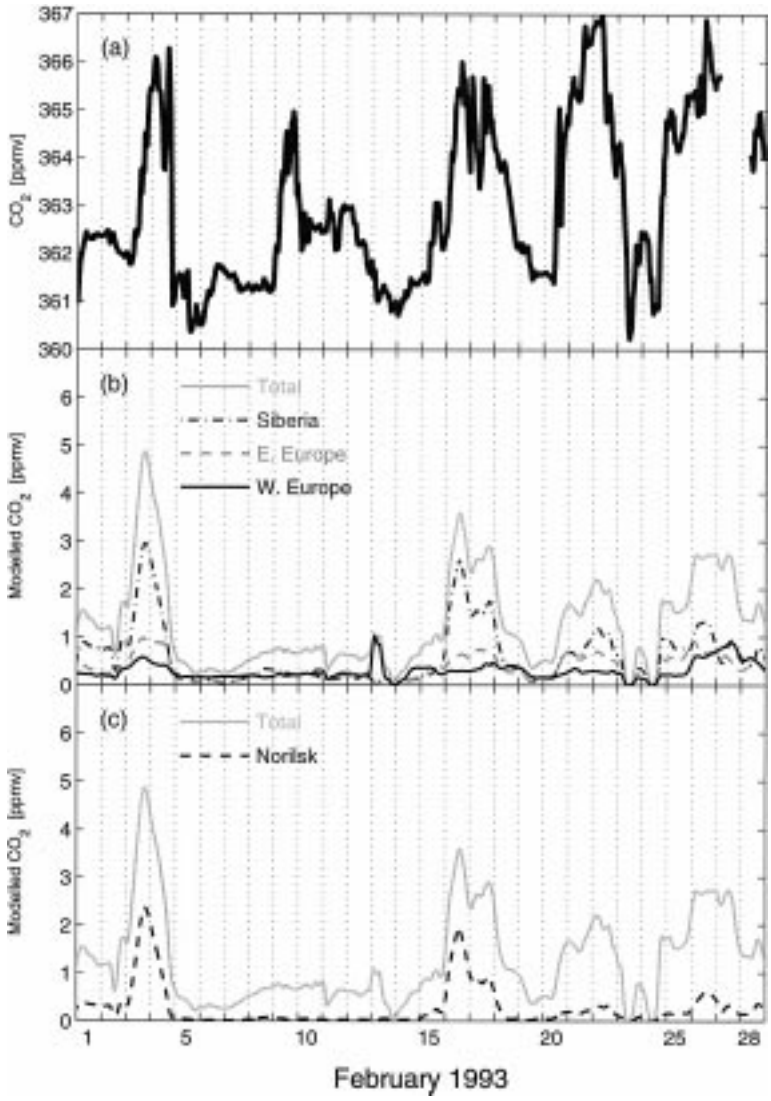

Fig. 5. Measured and modelled CO_2 at Zeppelinfjellet's location in February 1993. (a) Measured hourly median CO_2 mixing ratio. (b) Modelled CO_2 mixing ratio after 22 days of "harmonisation". Grey solid line is the results when using the scaled SO_x-emissions from Benkovitz et al. (1996) (1.9 Pg C year^{-1}). Dash-dotted line is the results of the Siberian emissions (0.36 Pg C year^{-1}), dashed line is from the east European emissions (0.44 Pg C year^{-1}), and black solid line is west European emissions (1.0 Pg C year^{-1}). (c) Modelled CO_2 mixing ratio after 22 days of "harmonisation". Solid line is the results when using the scaled SO_x-emissions from Benkovitz et al. (1996) (1.9 Pg C year^{-1}), dashed line is the scaled SO_x-emissions but with only the Norilsk source (0.08 Pg C year^{-1}) retained.

have, however, shown that Arctic haze typically occur in layers as thin as 50–100 m, and that the majority of the pollution is confined to the lowest 5 km of the troposphere (Shaw and Khalil, 1989). Clearly, the vertical resolution in MATCH is too coarse (layer thickness increasing from $\sim$50 m at surface to $\sim$500 m at 5 km) to resolve such thin layers and the modelled CO_2 anomalies at higher altitudes are therefore deemed to be of too small magnitude.

Inspection of maps (not shown) illustrating the simulated advection of the CO_2-plumes from Eurasia, show that the polluted air travelled in the lowest model layers during most of the transport from the emission regions to Spitsbergen. A prominent feature of MATCH is the effective mixing between the lowest few model layers. The modelled mixed layer height is thus always at least 200–250 m and any CO_2 that in the real world would be trapped in a shallower layer is effectively diluted. This, we believe, is the main reason for the too small amplitude of the simulated anomalies in late February, 1993.

5.3. *December 1994*

During other months the situation can be quite different. We have also performed simulations for October 1993 through January 1994 and November–December 1994. Below we briefly discuss the December 1994 case, which showed a situation with only small influence from the lower-Ob region but a marked influence from western Europe.

Fig. 7a shows measured CO_2 and σ_{sp} at Zeppelinfjellet in December 1994. Due to instrumental problems with the nephelometer, the accuracy and temporal resolution of σ_{sp} is lower than in previous periods. During this month one prominent CO_2 anomaly appeared around 9–10 December and a broader peak around 27–28 December. The CO_2 maxima were also discernible in the σ_{sp} record, which however, also displayed high values on 20 and 23 December (possibly caused by instrumental errors) without accompanying spikes in CO_2. Fig. 7b shows simulations, which only differ in the source function utilised. Both simulations were initiated with 0 ppmv CO_2 on 15 November.

The agreement between the observations and simulations is poorer than in the February 1993 case. Also, the difference between the two different source-fields at Zeppelinfjellet is much less. In fact, the CO_2 spike on the 9th it almost entirely due to the emissions originating in western Europe as can be seen in Fig. 7c which show the respective influence of the 3 regions and the Norilsk area discussed in Subsection 5.1. Vertical profiles (not shown) reveal similar features as the February 1993 case, i.e., the modelled, near-surface, CO_2 anomaly at Alert is of smaller magnitude than at Zeppelinfjellet. At higher levels, both over Zeppelinfjellet and over Alert we simulate CO_2 layers which stretches over several model levels but reaching only 1–2 ppmv in amplitude. The failure of simulating the actual magnitude is again attributed to the coarse vertical resolution and the inevitable numerical diffusion.

6. Summary and conclusions

We have used a regional transport model to simulate the advection of anthropogenic CO_2 through the Arctic troposphere during winter. The experimental design was based on the fact that weekly- to monthly-mean CO_2 mixing ratios only display small temporal and horizontal variations in the region during winter. This is a reflection of the relatively small natural CO_2 fluxes from underlying land and ocean during winter. By running the model with different initial fields and different boundary conditions we showed that most of the variability in CO_2 measured at a monitoring station on Spitsbergen was indeed caused by advection from anthropogenic sources within the model domain. The results are in contradiction to Yuen et al. (1996) who argue that 60% of a modelled CO_2 anomaly at Alert in the Canadian high Arctic was caused by biogenic CO_2 efflux from the Eurasian region. Given the high correlation between CO_2 and σ_{sp} during most of the CO_2 spikes at Spitsbergen we do not consider it likely that biogenic CO_2 efflux was a major CO_2 source during these episodes. A possible means to discriminate between anthropogenic and biogenic CO_2 flux from Siberia is to measure the $^{14}CO_2$:$^{12}CO_2$ ratio in atmospheric CO_2. Such studies are currently pursued at Zeppelinfjellet.

In our model, the CO_2 measurements at Spitsbergen were always as good, or better, reproduced when the CO_2 emissions within the model domain were distributed in proportion to the SO_x emissions instead of distributing them based on population density. We argue that the correlation with SO_x emissions is partly coincidental, and suggest that gas-exploitation in Siberia is an overlooked source for CO_2, and Arctic haze particles. This is supported by other measurements indicating high correlation between CO_2 and CH_4 during

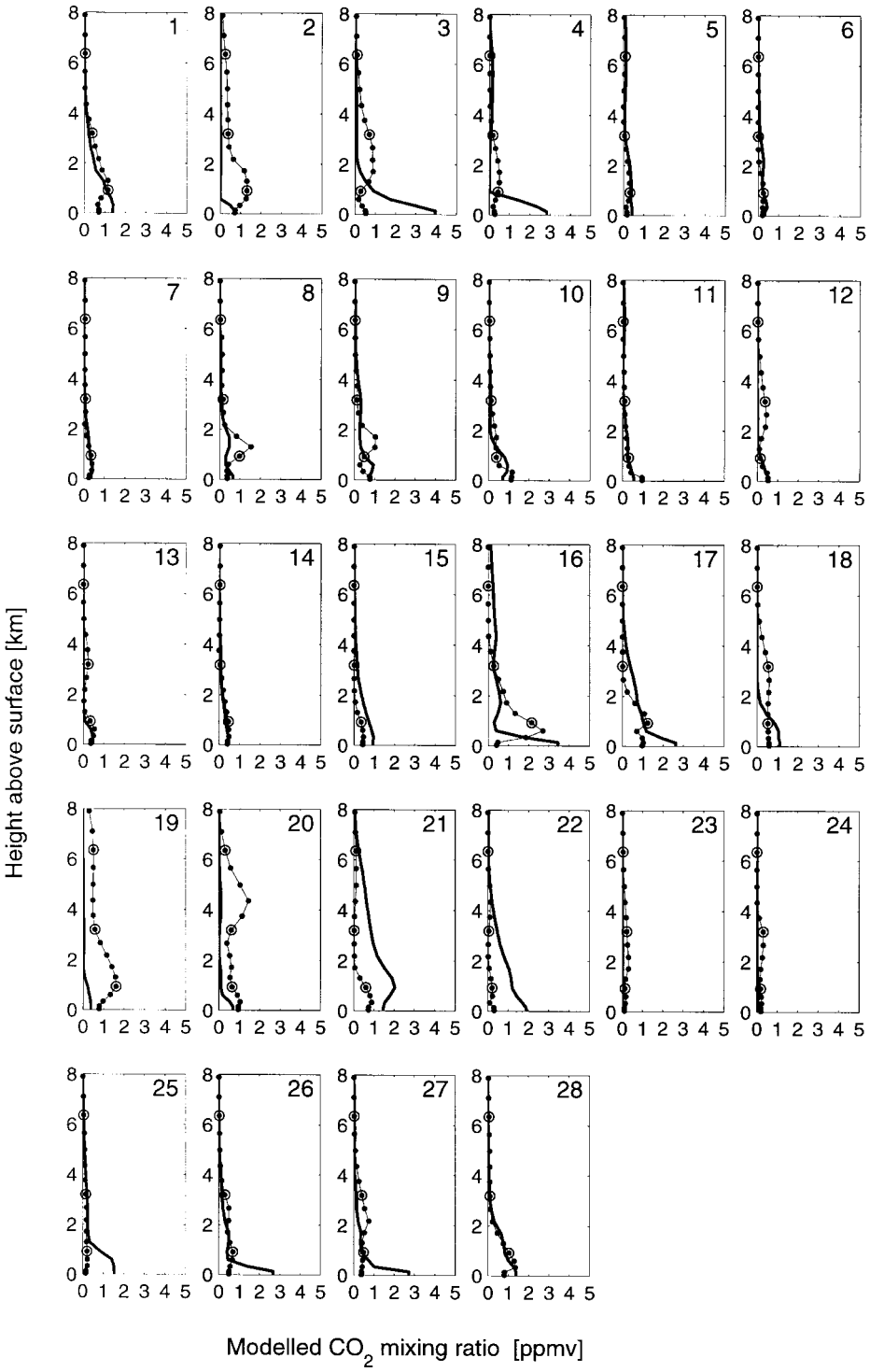
Height above surface [km]
Modelled CO_2 mixing ratio [ppmv]
1
2
3
4
5
6
7
8
9
10
11
12
13
14
15
16
17
18
19
20
21
22
23
24
25
26
27
28

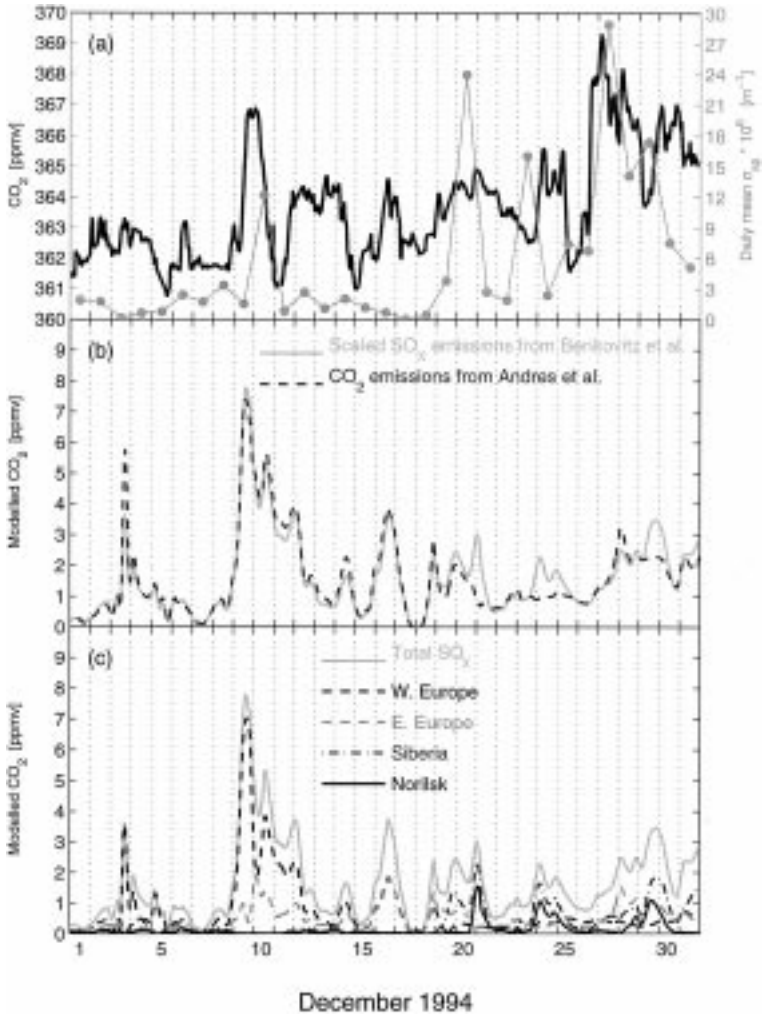

Fig. 7. Measured and modelled CO_2 at Zeppelinfjellet's location in December 1994. (a) Hourly median CO_2 mixing ratio (solid line). Also shown is daily mean σ_{sp} (dotted line). (b) Modelled CO_2 mixing ratio after 16 days of "harmonisation". Solid line is the results when using the scaled SO_x-emissions from Benkovitz et al. (1996), dashed line is with CO_2-emissions from Andres et al. (1996). Total CO_2 emissions in model domains is 1.9 Pg C year^{-1} in both simulations. (c) Modelled CO_2 mixing ratio after 16 days of "harmonisation". Grey solid line is the results when using the scaled SO_x-emissions from Benkovitz et al. (1996) (1.9 Pg C year^{-1}), black dashed line is west European emissions (1.0 Pg C year^{-1}), grey dashed line is from the east European emissions (0.44 Pg C year^{-1}), dash-dotted line is the results of the Siberian emissions (0.36 Pg C year^{-1}). Solid line is the scaled SO_x-emissions but with only the Norilsk source (0.08 Pg C year^{-1}) retained.

Fig. 6. Vertical profiles of modelled CO_2 mixing ratio during February 1993 at 1200 UTC the day indicated in the upper right corner of each panel. Solid line is instantaneous CO_2 mixing ratio over Zeppelinfjellet (79°N, 12°E), dotted line is instantaneous CO_2 profile over Alert (82°N, 62°W) in the Canadian Arctic. The results are taken from a run with the scaled SO_x-emissions from Benkovitz et al. (1996). Circles indicate model level 5, 10, 15; dots indicate intermediate levels.

Arctic haze episodes, although only the former has its main source during combustion.

We found that most of the transport to Spitsbergen takes place in the lowest km of the atmosphere, often following a path crossing both western and Eastern Europe before entering the Arctic from western Siberia. Although this study indicates that the Siberian sources around the gulf of Ob are of considerable importance for determining the amount of anthropogenic pollution in the Arctic during winter, the European sources also contribute significantly to Arctic haze pollutants. The respective sources absolute contribution remains to be quantified. Measurements of both CO_2 and aerosol particles close to the suspected emission regions would be most valuable for performing the quantitative studies.

The conclusions drawn here are based on only a few cases. In the future, more periods need to be studied, both episodes with direct transport from Europe without passing the lower-Ob region and cases where air is transported from Siberia, past the gulf of Ob. The biogenic CO_2 flux from Eurasia, which was not considered in this study, must clearly also be addressed. Such work is ongoing and will hopefully lead to a clearer picture of the role of the terrestrial biota and the lower-Ob gas-fields for Arctic haze events and the global carbon cycle.

Finally, we would like to stress that although the tongues of anthropogenic pollution from the lower-Ob region in western Siberia are only evident at a few locations at certain times of the year, the emissions may persist all year around. In this study, we find that up to 0.1 Pg C year^{-1}, or 8% of the total FSU emissions for 1990 are emitted near Norilsk. Since the air parcels take up some CO_2 en route to or from Norilsk, 0.1 Pg C year^{-1} is the maximum value supported by this study. It is probably unrealistically large even for the lower-Ob gas fields, but remains an indication of the uncertainty in current emission inventories. In another example, based on extrapolations of atmospheric CO_2 measurements in the plume from Prudhoe Bay, Brooks et al. (1997) estimated the CO_2 flux from the oil facilities to be 0.0114 Pg C year^{-1}, which is four times greater than the reported emissions from the oil facilities during the same time.

7. Acknowledgements

M. Heimann for providing boundary data. R. Andres and H. Rodhe for stimulating discussions and comments on earlier drafts of this manuscript. The European Commission (through the support of ESCOBA through contract ENV4-CT95–0116) and the Nordic Council of Ministers are acknowledged for financial support. The atmospheric monitoring activities performed by Stockholm University at Zeppelinfjellet are financed by the Swedish Environmental Protection Agency. Parts of this work were performed while M.E. spent a post doctoral year at CSIRO, Atmospheric Research, Aspendale, Australia.

8. Note added in proof

As a result of modelling studies conducted after acceptance of this paper, minor rewording was approved by the guest editor on 15 September 1998.

REFERENCES

Andres, R. J., Marland, G., Fung, I. and Matthews, E. 1996. A $1^\circ \times 1^\circ$ distribution of carbon dioxide emissions from fossil fuel consumption and cement manufacture, 1950–1990. *Global Biogeochem. Cycles* **10**, 419–429.

Barrie, L. A. 1986. Arctic air pollution: An overview of current knowledge. *Atmos. Environ.* **20**, 643–663.

Barrie, L. A. and Hoff, R. M. 1985. Five years of air chemistry observations in the Canadian Arctic. *Atmos. Environ.* **19**, 1995–2010.

Benkovitz, C. M., Scholtz, M. T., Pacyna, J., Tarrasón, L., Dignon, J., Voldner, E. C., Spiro, P. A., Logan, J. A. and Graedel, T. E. 1996. Global gridded inventories of anthropogenic emissions of sulfur and nitrogen. *J. Geophys. Res.* **101D**, 29239–29253.

Bolin, B. and Bischof, W. 1970. Variations of the carbon dioxide content of the atmosphere in the northern hemisphere. *Tellus* **22**, 431–442.

Bott, A. 1989a. A positive definite advection scheme obtained by nonlinear renormalization of the advective fluxes. *Mon. Wea. Rev.* **117**, 1006–1015.

Bott, A. 1989b. Reply. *Mon. Wea. Rev.* **117**, 2633–2636.

Brooks, S. B., Crawford, T. L. and Oechel, W. C. 1997. Measurements of carbon dioxide emissions plumes from Prudhoe Bay, Alaska oil fields. *J. Atmos. Chem.* **27**, 197–207.

Conway, T. J. and Steele, L. P. 1989. Carbon dioxide and methane in the Arctic atmosphere. *J. Atmos. Chem.* **9**, 81–99.

Conway, T. J., Steele, L. P. and Novelli, P. C. 1993. Correlations among atmospheric CO_2, CH_4 and CO in the Arctic, March 1989. *Atmos. Environ.* **27A**, 2881–2894.

Engardt, M., Holmén, K. and Heintzenberg, J. 1996. Short-term variations in atmospheric CO_2 at Ny-Ålesund, Spitsbergen, during spring and summer. *Tellus* **48B**, 33–43.

Hansen, A. D. A., Conway, T. J., Steele, L. P., Bodhaine, B. A., Thoning, K. W., Tans, P. and Novakov, T. 1989. Correlations among combustion effluent species at Barrow, Alaska: aerosol black carbon, carbon dioxide and methane. *J. Atmos. Chem.* **9**, 283–299.

Heimann, M. and Keeling, C. D. 1989. A 3-dimensional model of atmospheric CO_2 transport based on observed winds: 2. Model description and simulated tracer experiments. In: *Aspects of climate variability in the Pacific and the western Americas.* (ed. D. H. Peterson). American Geophysical Union, Washington, DC, USA, pp. 237–275.

Holmén, K., Engardt, M. and Odh, S.-Å. 1995. *The carbon dioxide measurement program at the Department of Meteorology at Stockholm University*. International Meteorological Institute in Stockholm, Report CM-84, 38 pp.

Holtslag, A. A. M., de Bruijn, E. I. F. and Pan, H.-L. 1990. A high resolution air mass transformation model for short-range weather forecasting. *Mon. Wea. Rev.* **118**, 1561–1575.

Holtslag, A. A. M., van Meijgaard, E. and de Rooy, W. C. 1995. A comparison of boundary layer diffusion schemes in unstable conditions over land. *Boundary-Layer Meteor.* **76**, 69–95.

Khalil, M. A. K. and Rasmussen, R. A. 1984. Statistical analysis of trace gases in Arctic haze. *Geophys. Res. Lett.* **11**, 437–440.

Levin, I., Graul, R. and Trivett, N. B. A. 1995. Long-term observations of atmospheric CO_2 and carbon isotopes at continental sites in Germany. *Tellus* **47B**, 23–34.

Marland, G., Andres, R. J. and Boden, T. A. 1994. Global, regional, and national CO_2 emissions. In: *Trends '93: a compendium of data on global change.* ORNL/CDIAC-65 (eds. T. A. Boden, D. P. Kaiser, R. J. Sepanski and F. W. Stoss). Carbon Dioxide Information Analysis Center, Oak Ridge National Laboratory, Oak Ridge, Tenn., USA, pp. 505–584.

Marland, G., Boden, T., Andres, R. J. and Johnston, C. 1998. *Estimates of global, regional, and national annual CO_2-emissions from fossil-fuel burning, hydraulic cement production, and gas flaring: 1751–1995*. Carbon Dioxide Information Analysis Center, Oak Ridge National Laboratory, Oak Ridge, Tenn., USA, NDP-030/R8.

McGrath, R. 1989. *Trajectory models and their use in the Irish Meteorological Service.* Irish Meteorological Service, Glasnevin Hill, Dublin, Internal Memorandum No. 112/89, 12 pp.

Müller, J.-F. 1992. Geographical distribution and seasonal variation of surface emissions and deposition velocities of atmospheric trace gases. *J. Geophys. Res.* **97D**, 3787–3804.

NOAA/CMDL. 1995. Atmospheric CO_2 monthly mean concentration: fixed NOAA flask network station. In: WMO WDCGG DATA REPORT. WDCGG No. 7. Japan Meteorological Agency, Tokyo, pp. 57–100.

NOAA/CMDL. 1996. Atmospheric CO_2 monthly mean concentration: fixed station NOAA flask sampling network. In: WMO WDCGG DATA REPORT. WDCGG No. 11. Japan Meteorological Agency, Tokyo, pp. 67–114.

Pacyna, J. M., Ottar, B., Tomza, U. and Maenhaut, W. 1985. Long-range transport of trace elements to Ny Ålesund, Spitsbergen. *Atmos. Environ.* **19**, 857–865.

Rotty, R. M. 1987. Estimates of seasonal variation in fossil fuel CO_2 emissions. *Tellus* **39B**, 184–202.

Robertson, L., Langner, J. and Engardt, M. 1998. An Eulerian limited area atmospheric transport model. *J. Appl. Meteor.* **38**, 190–210.

Shaw, G. E. and Khalil, M. A. K. 1989. Arctic haze. In: *The handbook of environmental chemistry*, vol. 4B. (ed. O. Hutzinger). Springer-Verlag, Berlin Heidelberg, pp. 69–111.

Tremback, C. J., Powell, J., Cotton, W. R. and Pielke, R. A. 1987. The forward-in-time upstream advection scheme: Extension to higher orders. *Mon. Wea. Rev.* **115**, 540–555.

Trivett, N. B. A., Worthy, D. E. J. and Brice, K. A. 1989. Surface measurements of carbon dioxide and methane at Alert during an Arctic haze event in April, 1986. *J. Atmos. Chem.* **9**, 383–397.

Waggoner, A. P. and Weiss, R. E. 1980. Comparison of fine particle mass concentration and light scattering extinction in ambient aerosol. *Atmos. Environ.* **14**, 623–626.

Worthy, D. E. J., Trivett, N. B. A., Hopper, J. F., Bottenheim, J. W. and Levin, I. 1994. Analysis of long-range transport events at Alert, Northwest Territories, during the Polar Sunrise Experiment. *J. Geophys. Res.* **99D**, 25329–25344.

Yamanouchi, T., Aoki, S., Morimoto, S. and Wada, M. 1996. Report on atmospheric science observations at Ny-Ålesund, Svalbard. *Mem. Natl Inst. Polar Res.* (Spec. Issue) **51**, 153–163.

Yuen, C. W., Higuchi, K., Trivett, N. B. A. and Cho, H.-R. 1996. A simulation of a large positive CO_2 anomaly over the Canadian Arctic archipelago. *J. Meteor. Soc. Japan* **74**, 781–795.

Zilitinkevich, S. and Mironov, D. V. 1996. A multi-limit formulation for the equilibrium depth of a stably stratified boundary layer. *Boundary-layer Meteor.* **81**, 325–351.

Zimov, S. A., Davidov, S. P., Voropaev, Y. V., Prosiannikov, S. F., Semiletov, I. P., Chapin, M. C. and Chapin, F. S. 1996. Siberian CO_2 efflux in winter as a CO_2 source and cause of seasonality in atmospheric CO_2. *Climatic Change* **33**, 111–120.